REVISTA DE LA
UNIÓN MATEMÁTICA ARGENTINA
Volumen 47, Número 2, 2006, Páginas 137–150

BIFURCATION THEORY AND THE HARMONIC CONTENT OF OSCILLATIONS

GRISELDA R. ITOVICH, FEDERICO I. ROBBIO AND JORGE L. MOIOLA

Abstract. The harmonic content of periodic solutions in ODEs is obtained using standard techniques of harmonic balance and the fast Fourier transform (FFT). For the first method, the harmonic content is attained in the vicinity of the Hopf bifurcation condition where a smooth branch of oscillations is born under the variation of a distinguished parameter. The second technique is applied directly to numerical simulation, which is assumed to be the correct solution. Although the first method is local, it provides an excellent tool to characterize the periodic behavior in the unfoldings of other more complex singularities, such as the double Hopf bifurcation (DHB). An example with a DHB is analyzed with this methodology and the FFT algorithm.

1. INTRODUCTION

The Hopf bifurcation theorem (HBT) provides a key tool to determine the birth of periodic solutions in nonlinear differential equations which depend on a distinguished parameter [3,5]. Furthermore, the HBT not only constitutes an elegant analytical treatment to assure the existence of oscillations as well as their stability but also supplies formulas to approximate locally the harmonic content of the oscillations [8,9]. Although the expressions for approximating the periodic solutions can be obtained by using different analytical techniques [13,7], a special consideration is assigned to harmonic balance methods (HBM) due to its tradition in mechanical and electrical engineering [15,2,1]. More specifically, one can separate the scope of the method in terms of the number of computed harmonics. For example, in [15] the authors have the objective of determining the stability of the periodic solutions and its bifurcations by using the information of the first harmonic given, at the same time, a simple test in engineering terms. On the opposite, in [2] the authors have computed up to twenty harmonics in order to detect carefully the tortuosity of the periodic solution branch in terms of the distinguished

Key words and phrases. Double Hopf bifurcation, Harmonic balance, Limit cycles.
GRI acknowledges Universidad Nacional del Comahue.
FIR and JLM acknowledge CONICET (PIP 5032), Universidad Nacional del Sur (24/K030) and PICT-11-12524 of the ANPCyT.

bifurcation parameter. In the middle of both extremes, in [10] the authors have presented the approximation of the periodic solutions from Hopf bifurcation with two, four, six and eight harmonics. This approach gives a reasonable complexity in the computation and a respectable accuracy in the neighborhood of the bifurcation point. This article intends to explore an accurate measure of the first harmonics (up to order eight) based on the approximation formulas obtained in [10], but in this case applied to a double resonant circuit [16,4]. In electronic terms, the purity of a sinusoidal oscillator is defined as the ratio between the amplitude of the total harmonic content to the amplitude of the first harmonic component. This magnitude can be *sensed* graphically by electronic circuit designers [6,12] by ordering the amplitude of the different harmonics with the HBM and the Fast Fourier Transform (FFT) technique [11] evaluated on the numerical solution of the ODE. This paper is organized as follows: the background of Hopf bifurcation in the frequency domain [8] is briefly reviewed in Section 2 and a summary of results about stability and bifurcation of cycles can be found in Section 3. In Section 4, a double resonant nonlinear circuit is analyzed and its harmonic content with both methods is compared. The conclusions are reported in Section 5.

2. BASIC CONCEPTS

Let us consider an n-dimensional nonlinear differential system expressed by

$$\dot{x} = f(x;\mu), \tag{1}$$

where $\dot{x} = \frac{dx}{dt}$, $x \in R^n$, $f \in C^r$, $r \geq 9$ and $\mu \in R$ is a bifurcation parameter. It is supposed that $\tilde{x}$ is an equilibrium point ($f(\tilde{x};\mu) = 0$) of (1). This system can be also written via input and output variables, namely $u \in R^p$ and $y \in R^m$, as a feedback control problem. Thus, one obtains the following mixed representation with a state variable x, an output variable y, and a nonlinear control u

$$\begin{aligned} \dot{x} &= Ax + B[Dy + u], \\ y &= Cx, \\ u &= g(e;\mu) = \tilde{g}(y;\mu) - D(\mu)y, \end{aligned} \tag{2}$$

where A is a $n \times n$ matrix, B is $n \times p$, C is $m \times n$ and D is $p \times m$. All matrices can depend on μ, $\tilde{g}$ is a nonlinear function defined on R^p which results from the original function f and the selection made for the matrices A, B, C and D, besides $g \in C^r$, $r \geq 9$, where $e = -y$. Then, if one applies Laplace transform to system (2) with the initial condition $x(0) = 0$, the analysis of the feedback system proceeds by finding the equilibrium $\tilde{e}$, which is the solution of the equation

$$e = -G(0;\mu)g(e;\mu), \tag{3}$$

where $G(s;\mu) = C[s*I-(A+BDC)]^{-1}B$ is the transfer matrix of the linear part of system (2), s being the Laplace transform variable, and a nonlinear part represented by $u = g(e;\mu)$ which can be thought of as an input of the system. Computing a linearization of (2) at the equilibrium $\tilde{e}$, one obtains a system whose Jacobian J is a $p \times m$ matrix given by

$$J = J(\mu) = D_1 g(e;\mu)|_{e=\tilde{e}} = \left[\left. \frac{\partial g_j}{\partial e_k} \right|_{e=\tilde{e}} \right], \tag{4}$$

where $g = \begin{bmatrix} g_1 & g_2 & \cdots & g_p \end{bmatrix}^T$, $j = 1,2,\cdots,p$, $k = 1,2,\cdots,m$. Then, the application of the generalized Nyquist stability criterion [8] provides the necessary conditions for the critical cases:

Lemma 1: If the linearization of system (1) evaluated at $\tilde{x}$ has an eigenvalue $i\omega_0$ when $\mu = \mu_0$ then the associated eigenvalue of the matrix $G(i\omega_0;\mu_0)J(\mu_0)$ evaluated at $\tilde{e}$ takes the value $(-1+i0)$ for $\mu = \mu_0$.

The situation of Lemma 1 concerns the existence of bifurcations in the solutions of system (1). If $\omega_0 \neq 0$ and some additional conditions are satisfied [10], a Hopf bifurcation arises. This is related to the appearance or disappearance of periodic solutions.

Due to Lemma 1, it is known that if a bifurcation exists in (1) then

$$h(-1,i\omega;\mu) = \det(-1*I - G(i\omega;\mu)J(\mu)) = 0, \tag{5}$$

for a certain pair (ω_0,μ_0). The equation (5) can be transformed by splitting its real (Re) and imaginary (Im) parts as written below

$$\begin{cases} F_1(\omega,\mu) = \mathrm{Re}(h(-1,i\omega;\mu)) = 0, \\ F_2(\omega,\mu) = \mathrm{Im}(h(-1,i\omega;\mu)) = 0. \end{cases}$$

Making use of the functions F_1 and F_2, the next result can be formulated [9]:

Proposition 1: If a Hopf bifurcation exists at (ω_0,μ_0), $\omega_0 \neq 0$, then it follows:

$$F_1(\omega_0,\mu_0) = F_2(\omega_0,\mu_0) = 0.$$

The HBT [3,5] gives sufficient conditions to assure the appearance of a branch of periodic solutions in (1). Its formulation in the frequency domain [8,9,10] is established through three fundamental hypotheses:

Theorem 1:
H1) There is a unique complex function $\hat{\lambda}$, which solves $h(\lambda, i\omega; \mu) = 0$, passes through $(-1 + i0)$ with frequency $\omega_0 \neq 0$ and $\mu = \mu_0$ and involves a stability change of the equilibrium while varying the parameter μ. Moreover, $\frac{\partial F_1}{\partial \omega}\Big|_{(\omega_0,\mu_0)}$, $\frac{\partial F_2}{\partial \omega}\Big|_{(\omega_0,\mu_0)}$ do not vanish simultaneously, avoiding any resonance case.

H2) The determinant M_1 is nonzero, i.e.

$$M_1 = \left| \frac{\partial(F_1, F_2)}{\partial(\omega, \mu)} \Big|_{(\omega_0,\mu_0)} \right| = \begin{vmatrix} \frac{\partial F_1}{\partial \omega} & \frac{\partial F_1}{\partial \mu} \\ \frac{\partial F_2}{\partial \omega} & \frac{\partial F_2}{\partial \mu} \end{vmatrix}_{(\omega_0,\mu_0)} \neq 0,$$

which is an equivalent expression for the nondegeneracy of the transversality condition of the classic formulation in the time domain.

H3) The expression σ_1, known as stability or curvature coefficient, and given by

$$\sigma_1 = -\operatorname{Re}\left(\frac{u^T G(i\omega_0; \mu_0) p_1(\omega_0, \mu_0)}{u^T G'(i\omega_0; \mu_0) J(\mu_0) v} \right), \tag{6}$$

has a sign definition. This coefficient can be calculated by other techniques and is also recognized as the first Lyapunov coefficient [5].

Observation: In the last formula, u^T and v are the left and right normalized eigenvectors of the matrix $G(i\omega_0; \mu_0)J(\mu_0)$ associated with the eigenvalue $\hat{\lambda}$ ($\bar{u}^T v = 1$ and $\bar{v}^T v = 1$, where " $\bar{\cdot}$ " means complex conjugate), $G' = \frac{dG}{ds}$ and p_1 is a p-dimensional complex vector

$$p_1(\omega, \mu) = QV_{02} + \frac{1}{2}\overline{Q}V_{22} + \frac{1}{8}L\overline{v},$$

whose computation is based on the second and third derivatives of the function g [8], and Q, $\overline{Q}$ and L are $p \times m$ matrices defined as

$$Q = Q(\mu) = D_2 g(e; \mu)|_{e=\tilde{e}} = \left[\sum_{l=1}^{m} \frac{\partial^2 g_j}{\partial e_l \partial e_k}\Big|_{\tilde{e}} v_l \right],$$

where $v = \begin{bmatrix} v_1 & v_2 & \cdots & v_m \end{bmatrix}^T$, and

$$L = L(\mu) = D_3 g(e; \mu)|_{e=\tilde{e}} = \left[\sum_{l=1}^{m} \sum_{i=1}^{m} \frac{\partial^3 g_j}{\partial e_l \partial e_i \partial e_k}\Big|_{\tilde{e}} v_l v_i \right],$$

where $j = 1, 2, \cdots, p$, $k = 1, 2, \cdots, m$. Furthermore, the following vectors are defined

$$V_{02} = -\frac{1}{4}H(0; \mu)Q\overline{v}, \quad V_{22} = -\frac{1}{4}H(i2\omega; \mu)Qv,$$

where $H(s;\mu) = [I + G(s;\mu)J(\mu)]^{-1} G(s;\mu)$ is the so-called closed loop transference matrix.

Then a branch of periodic solutions starts at $\mu = \mu_0$ whose direction and stability result from the values of M_1 and σ_1, respectively. When $\sigma_1 > 0$ it follows that the solution will be unstable (subcritical Hopf bifurcation) or else stable if $\sigma_1 < 0$ (supercritical case).

The demonstration of the HBT by using harmonic balance is constructive, namely, it allows to write an approximate expression of the periodic solution, after estimating its frequency ω and the amplitude θ of its first harmonics. These values can be interpreted as a part of a certain graphic in the complex plane and this is the reason for calling this formulation as the graphical Hopf theorem. More specifically, according with the behavior of the eigenlocus described by the critical eigenvalue $\hat{\lambda} = \hat{\lambda}(i\omega;\mu)$, one chooses $\tilde{\mu}$ next to μ_0 and searches for a first estimate of the frequency $\tilde{\omega}$, through the intersection point between the eigenlocus and the real axis, which results nearest to $(-1 + i0)$. With this solution pair $(\tilde{\omega}, \tilde{\mu})$, one computes the corresponding eigenvectors u^T, v, the vector p_1 and the complex number $\xi_1 = -u^T G(i\tilde{\omega};\tilde{\mu})p_1$. Then, a certain curve is plotted, described by $L_1 = -1+\xi_1\theta^2$, as θ varies, which is known as the *amplitude locus*. The next step consists in looking for the intersection between the two mentioned loci. So, one obtains a new solution pair $(\hat{\omega}, \hat{\theta})$, where $\hat{\omega} = \hat{\omega}(\tilde{\mu})$ and $\hat{\theta} = \hat{\theta}(\tilde{\mu})$ are approximations for the frequency and the amplitude of the analyzed oscillation. Using second order harmonic balance, one calculates a semi-analytical approximate expression of the variable e which appears in the system (2) writing

$$e = e(t;\tilde{\mu}) = \tilde{e}(\tilde{\mu}) + \mathrm{Re}\left(\sum_{k=0}^{2} E_k \exp(ik\hat{\omega}t)\right), \tag{7}$$

where $E_0 = \hat{\theta}^2 V_{02}$, $E_1 = \hat{\theta} v + \hat{\theta}^3 V_{13} = \hat{\theta} V_{11} + \hat{\theta}^3 V_{13}$, $E_2 = \hat{\theta}^2 V_{22}$. The vector V_{13} can be found by solving

$$P[I + G(i\hat{\omega};\tilde{\mu})J(\tilde{\mu})]V_{13} = -PG(i\hat{\omega};\tilde{\mu})p_1, \tag{8}$$

where $P = I - V_{11}V_{11}^T$, under the condition $V_{13} \perp V_{11}$. All the previous expressions which involve the nonlinear function g must be evaluated at the equilibrium $\tilde{e} = \tilde{e}(\tilde{\mu})$. The generalization of the described method with explicit fourth-order harmonic balance formulas appears in [9] and justifies the properties established for $f(.)$ at the beginning of this section, which are inherited by the function $g(.)$. This extension allows to improve the approximations substantially, due to the use of better estimations of the frequency and amplitude of the oscillation. The details and explicit expressions for the computation involving up to eight harmonics ($q = 4$, in the equation below) can be found in [10] and repeated here briefly as

$$e(t) = \tilde{e}(\tilde{\mu}) + \mathrm{Re}\left\{\sum_{k=0}^{2q} E_k \exp(ik\hat{\omega}t)\right\}, \tag{9}$$

where $E_0 = \hat{\theta}^2 V_{02} + \hat{\theta}^4 V_{04} + \hat{\theta}^6 V_{06} + \cdots + \hat{\theta}^{2q} V_{0,2q}$, $E_1 = \hat{\theta} V_{11} + \hat{\theta}^3 V_{13} + \hat{\theta}^5 V_{15} + \cdots + \hat{\theta}^{2q+1} V_{1,2q+1}$, $E_2 = \hat{\theta}^2 V_{22} + \hat{\theta}^4 V_{24} + \hat{\theta}^6 V_{26} + \cdots + \hat{\theta}^{2q} V_{2,2q}$ and $E_k = \hat{\theta}^k V_{kk} + \hat{\theta}^{k+2} V_{k,k+2} + \cdots + \hat{\theta}^{2q} V_{k,2q}$.

However, one must keep in mind that these results are valid locally (the parameter μ must be close to the Hopf bifurcation value μ_0) and when the analyzed cycles have small amplitude.

3. STABILITY OF CYCLES

Floquet theory can be applied to examine the stability of a periodic solution $\mathbf{X} = \mathbf{X}(t; \tilde{\mu})$ of a system as (1) [5,15]. The stability of the orbit $\mathbf{X}$ is based on the study of the eigenvalues of the so-called monodromy matrix. This array is obtained from the general solution of the following differential equation

$$\dot{z} = D(t)z, \tag{10}$$

where $z \in R^n$, $\dot{z} = \frac{dz}{dt}$ and $D(t) = D_1 f(\mathbf{X}(t; \tilde{\mu}); \tilde{\mu}) = \left.\frac{\partial f}{\partial x}\right|_{x=\mathbf{X}(t;\tilde{\mu}),\mu=\tilde{\mu}}$, $D(t+T) = D(t)$, T being the period of the cycle $\mathbf{X}$.

If one considers $M = M(t)$, a fundamental matrix of solutions of (10) such as $M(0) = I$, where I is the identity of order n, and computes $M(T)$, then the *monodromy matrix* of the orbit $\mathbf{X}$ is obtained. The eigenvalues of this matrix are known as Floquet or characteristic multipliers. It can be proved that one of the multipliers of a periodic solution of an autonomous system is always identically $+1$ and it gives a theoretical measure for the accuracy of the cycle approximation. Then, if all Floquet multipliers except the one at $+1$ are inside the unit circle, the limit cycle is stable.

If one or more Floquet multipliers are crossing the unit circle after a parameter variation, the periodic solution changes its stability. Generally, this situation gives rise to a bifurcation of cycles. There are three possibilities of crossing as shown in Figure 1: a) One multiplier crosses the border along the negative real axis (crosses by -1), b) one multiplier traverses the unit circle through the positive real axis

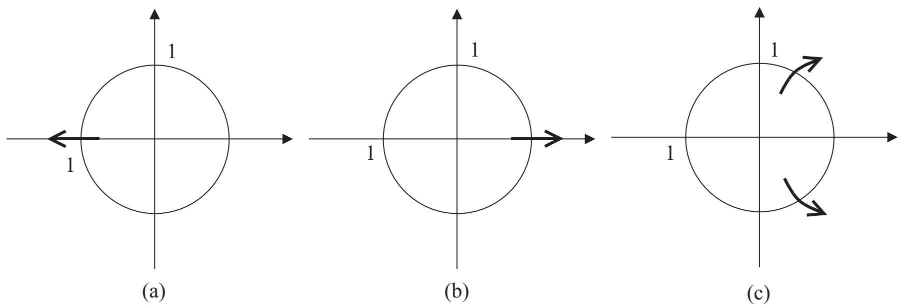

FIGURE 1. Bifurcations of cycles: (a) flip or period-doubling, (b) fold, transcritical or pitchfork, (c) Neimark-Sacker.

(crosses by +1), and c) two complex conjugate multipliers cross simultaneously the frontier out of the real axis. In case (a), a flip or period-doubling bifurcation of cycles appears, giving rise to a new periodic solution that rests over a Möbius band in R^n [14] and whose period doubles the period of the orbit $\mathbf{X}$. On the contrary, case (b) results in fold (saddle-node), transcritical or pitchfork (symmetry-breaking) bifurcation [5]. Finally, in case (c) a secondary Hopf or Neimark-Sacker bifurcation occurs and, in its vicinity, a quasiperiodic motion can be detected. In this work, besides the trivial multiplier +1 another complementary measure will be introduced considering the harmonic content of the approximated cycle and the one obtained by numerical simulation.

4. EXAMPLE

The considered nonlinear system describes two coupled circuits LCR as shown in Figure 2, where C_1, C_2 are capacitors, L_1, L_2 are inductances, and R is a resistor. The conductance is a nonlinear element which is described through the current-voltage relation as: $i_G = -\frac{1}{2}v_G + v_G^3$. If the voltages across the capacitors and the currents in the inductors are chosen as the state variables, it follows

$$
\begin{aligned}
\dot{x}_1 &= \tfrac{1}{2}\eta_1 x_1 + \eta_1 x_2 - \eta_1 x_4 - \eta_1 x_1^3, \\
\dot{x}_2 &= -\tfrac{1}{2}\sqrt{2}\, x_1, \\
\dot{x}_3 &= (\sqrt{2}+1)x_4, \\
\dot{x}_4 &= (2-\sqrt{2})(x_1 - x_3 - \eta_2 x_4),
\end{aligned}
\tag{11}
$$

where $x = (x_1, x_2, x_3, x_4) = (v_{C_1}, i_{L_1}, v_{C_2}, i_{L_2})$, $\eta_1 = \frac{1}{C_1}$ and $\eta_2 = R$ are two independent bifurcation parameters, and $C_2 = \sqrt{2}-1$, $L_1 = \sqrt{2}$ and $L_2 = \frac{1}{2}(2+\sqrt{2})$. It is easy to see that the unique equilibrium point of Sys. (11) is $\tilde{x} = 0$. In [16], the

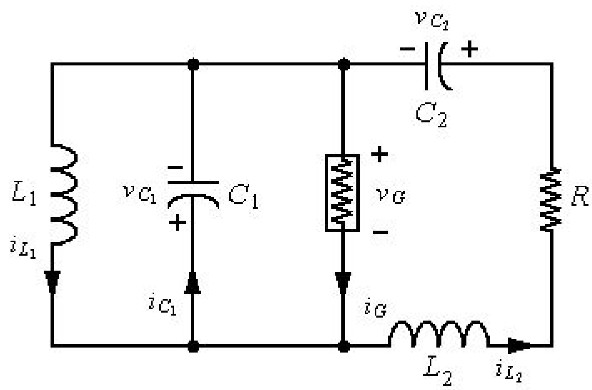

FIGURE 2. Double resonant circuit [16].

existence of a non-resonant double Hopf bifurcation with frequencies $\omega_1 = 1$ and $\omega_2 = \sqrt{2}$ for $\eta_1 = 2$ and $\eta_2 = 1 + \frac{1}{2}\sqrt{2}$, is shown. It must be taken into account that this Hopf degeneracy is a singularity of codimension 2, i.e., its unfolding is dynamically characterized by two parameters. Then, the HBM is applied to each Hopf bifurcation curve in order to recover the periodic solution branches.

It is proposed the following feedback realization of Sys. (11)

$$\begin{aligned} \dot{x} = &\quad Ax + B(Dy + u), \quad y = Cx, \\ u = &\quad g(e) = \tilde{g}(y) - Dy, \end{aligned}$$

where

$$A = \begin{bmatrix} 0 & \eta_1 & 0 & -\eta_1 \\ -\frac{1}{2}\sqrt{2} & 0 & 0 & 0 \\ 0 & 0 & 0 & \sqrt{2}+1 \\ 2-\sqrt{2} & 0 & -(2-\sqrt{2}) & -(2-\sqrt{2})\eta_2 \end{bmatrix},$$

$$C = \begin{bmatrix} 1 & 0 & 0 & 0 \end{bmatrix}, \quad B = -C^T \quad \text{and} \quad D = [\ 0\ ], \tag{12}$$

$u = g(e) = \eta_1 \left(-\frac{1}{2}e + e^3\right)$, with $e = -y$.

Thus, calculating the matrix G, that in this case is only a scalar, Eq. (3) yields $\tilde{e} = 0$ and the Jacobian J results $J = -\frac{\eta_1}{2}$. Therefore, the characteristic eigenvalue $\hat{\lambda}$ is obtained through the matrix GJ when it is evaluated for $s = i\omega$, namely

$$\hat{\lambda} = (A_1 + iA_2)\ (A_3 + iA_4)^{-1},$$

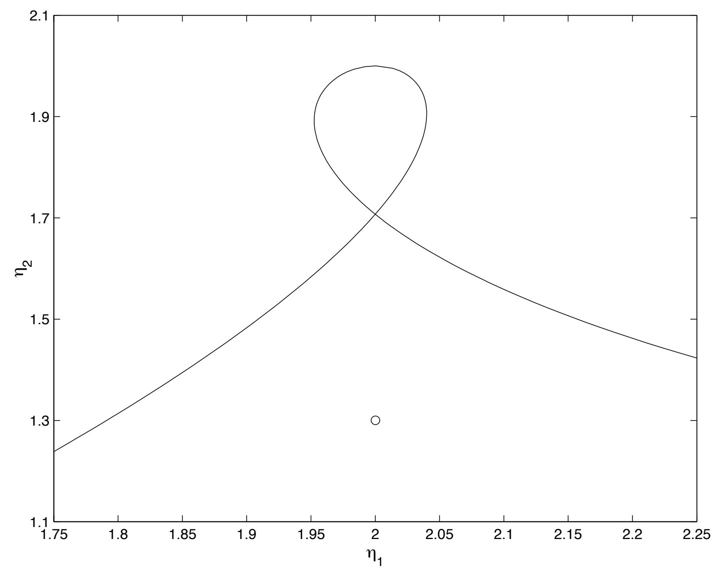

FIGURE 3. Hopf bifurcation curve for Sys. (11). ((o) $(\eta_1, \eta_2) = (2, 1.3)$)

where

$$A_1 = -\eta_1\eta_2\omega^2(2-\sqrt{2}),$$
$$A_2 = \eta_1\omega(\sqrt{2}-\omega^2),$$
$$A_3 = -2\omega^4 + \kappa\omega^2 - 2\eta_1,$$
$$A_4 = (4-2\sqrt{2})\eta_2\omega^3 - (2\sqrt{2}-2)\eta_1\eta_2\omega,$$

with $\kappa = (4-\sqrt{2})\eta_1 + 2\sqrt{2}$. Solving the nonlinear system $F_1(\omega, \eta) = \mathrm{Re}(\hat{\lambda}) + 1 = 0$, $F_2(\omega, \eta) = \mathrm{Im}(\hat{\lambda}) = 0$, where $\eta = (\eta_1, \eta_2)$, the Hopf bifurcation points are obtained and its graphical representation in the parameter space η is given in Figure 3. The selfcrossing of this curve is the non-resonant DHB mentioned previously. By varying the parameters η_1 and η_2 around the Hopf bifurcation curve, Sys. (11) exhibits diverse dynamic behaviors [4]. Particularly, when $\eta_1 = 2$ and $\eta_2 = 1.3$ two stable cycles coexist, one for each periodic branch, and they are shown in Figure 4.

If the initial condition is chosen close to the origin, the small limit cycle is reached whereas the larger one is achieved starting with an initial condition farther from equilibrium. With the HBM of eighth order it is possible to estimate the first

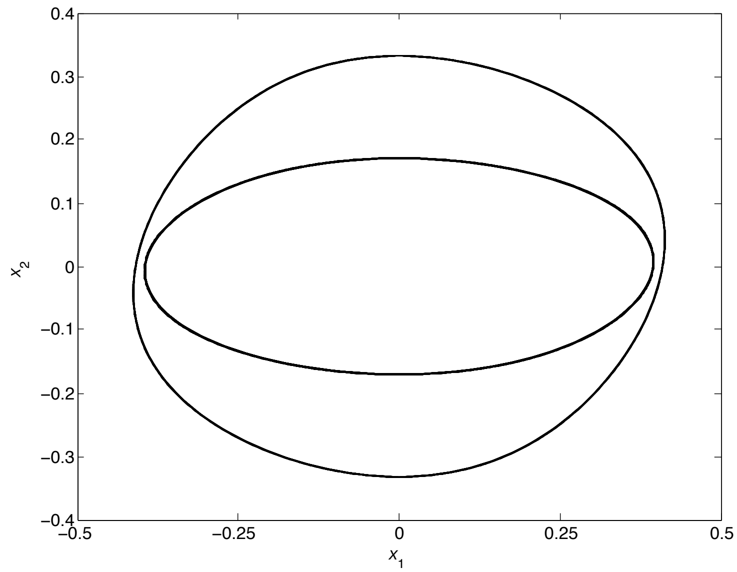

FIGURE 4. Two stable limit cycles for Sys. (11) with $(\eta_1, \eta_2) = (2, 1.3)$.

component of the limit cycle as

$$\begin{aligned} x_1(t) &= a_0 \cos(\hat{\omega}_2 t) + a_1 \cos(3\hat{\omega}_2 t) + a_2 \sin(3\hat{\omega}_2 t) + a_3 \cos(5\hat{\omega}_2 t) + \\ &\quad a_4 \sin(5\hat{\omega}_2 t) + a_5 \cos(7\hat{\omega}_2 t) + a_6 \sin(7\hat{\omega}_2 t), \end{aligned}$$

where $a_0 = -0.39476619$, $a_1 = -0.77433989 \times 10^{-3}$, $a_2 = 0.69648608 \times 10^{-2}$, $a_3 = 0.21638611 \times 10^{-3}$, $a_4 = 0.27356940 \times 10^{-4}$, $a_5 = 0.30154649 \times 10^{-5}$, $a_6 = -0.60240323 \times 10^{-5}$ and the fundamental frequency is $\hat{\omega}_2 = 1.63176876$. In this case, the eigenvalues of the monodromy matrix are: $\lambda_1 = 0.99996918$, $\lambda_2 = 0.57538276$, and $\lambda_{3,4} = 0.8480e^{\pm i3.0768}$. The results with the HBM are shown in the upper part of Figure 5, while its lower part depicts the complete harmonic content of the numerical simulation of the original system. Both waveforms are obtained through FFT techniques for an easy comparison.

The first component of the other limit cycle with fundamental frequency $\hat{\omega}_1 = 0.86081428$ is expressed through

$$\begin{aligned} x_1(t) &= a_0 \cos(\hat{\omega}_1 t) + a_1 \cos(3\hat{\omega}_1 t) + a_2 \sin(3\hat{\omega}_1 t) + a_3 \cos(5\hat{\omega}_1 t) + \\ &\quad a_4 \sin(5\hat{\omega}_1 t) + a_5 \cos(7\hat{\omega}_1 t) + a_6 \sin(7\hat{\omega}_1 t), \end{aligned}$$

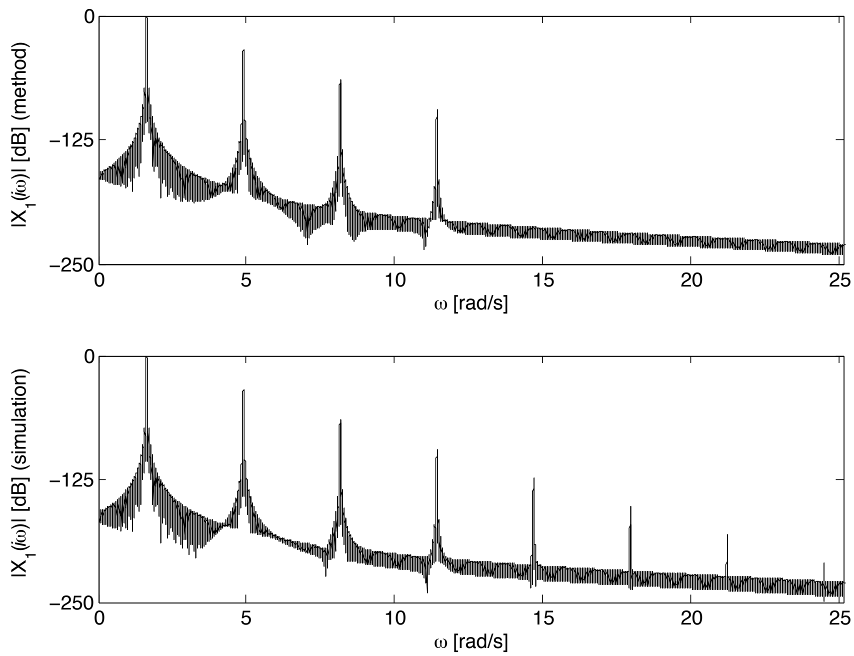

FIGURE 5. Harmonic content of the small limit cycle with fundamental frequency $\hat{\omega}_2 = 1.63176876$ for $(\eta_1, \eta_2) = (2, 1.3)$.

where $a_0 = -0.40598360$, $a_1 = -0.42186586 \times 10^{-2}$, $a_2 = 0.21408871 \times 10^{-1}$, $a_3 = 0.16248559 \times 10^{-2}$, $a_4 = 0.55248524 \times 10^{-3}$, $a_5 = 0.79656378 \times 10^{-4}$, $a_6 = -0.49948418 \times 10^{-4}$ and the Floquet multipliers are: $\lambda_1 = 1.00035562$, $\lambda_2 = 0.61353938$, and $\lambda_{3,4} = 0.4989e^{\pm i0.1406}$. In both cases the even harmonics are zero, and the agreement between both techniques is impressive, at least up to the seventh-order harmonics (see Figure 6). Notice, however, that harmonics higher to the seventh-order are smaller than one-thousandth to the first harmonics, and so their contribution in engineering terms is negligible.

5. CONCLUSIONS

The harmonic content of periodic solutions in ODEs has been obtained using two different techniques: one enrooted in the classical analysis of bifurcation theory and the other coming from numerical simulation. The first technique is able to recover up to the eighth harmonics via a HBM, while the second gives the complete spectrum obtained directly from numerical simulations. The agreement between

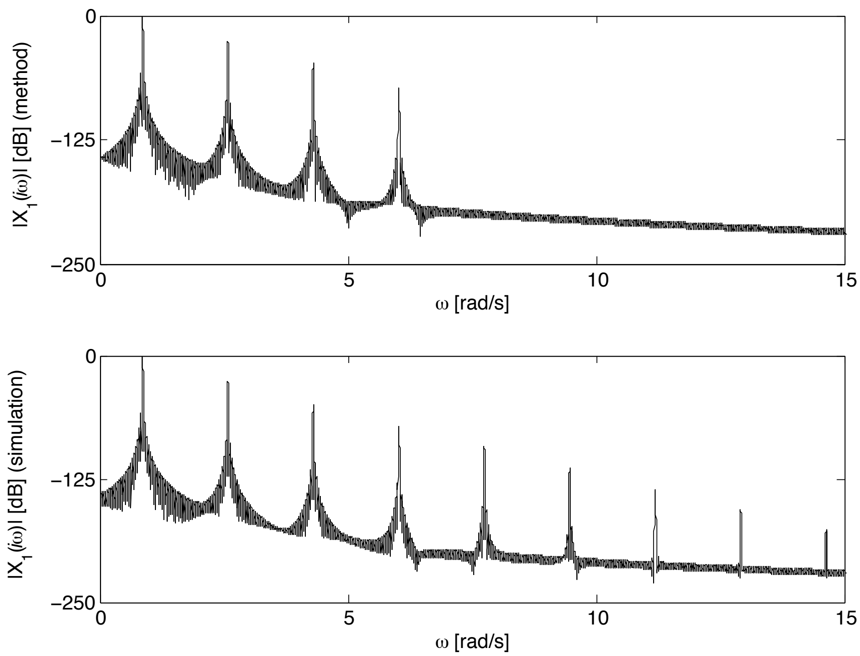

FIGURE 6. Harmonic content of the big limit cycle with fundamental frequency $\hat{\omega}_1 = 0.86081428$ for $(\eta_1, \eta_2) = (2, 1.3)$.

results coming from these two different methods is amazing, at least close to the Hopf bifurcation curve. Moreover, the HBM has allowed to analyze the dynamic behavior in the unfolding of a DHB accurately.

References

[1] Berns DW, Moiola JL, Chen, G. Detecting period-doubling bifurcation: an approximate monodromy matrix approach. Automatica 37, No.11, 1787-1795 (2001).

[2] Bonani F, Gilli M. Analysis of stability and bifurcations of limit cycles in Chua's circuit through the harmonic-balance approach. IEEE Trans. Circuits Syst., I, Fundam. Theory Appl. 46, No.8, 881-890 (1999).

[3] Hale J, Koçak H. Dynamics and bifurcations. New York: Springer-Verlag; 1991.

[4] Itovich G, Moiola JL. Double Hopf bifurcation analysis using frequency domain methods. Nonlinear Dyn. 39, No.3, 235-258 (2005).

[5] Kuznetsov YA. Elements of applied bifurcation theory. New York: Springer-Verlag; 1995.

[6] Maggio GM, De Feo O, Kennedy MP. Nonlinear analysis of the Colpitts oscillator and applications to design. IEEE Trans. Circuits Syst., I, Fundam. Theory Appl. 46, No.9, 1118-1130 (1999).

[7] Maggio GM, De Feo O, Kennedy MP. A general method to predict the amplitude of oscillation in nearly sinusoidal oscillator. IEEE Trans. Circuits Syst., I, Fundam. Theory Appl. 51, No.8, 1586-1595 (2004).

[8] Mees AI, Chua L. The Hopf bifurcation theorem and its applications to nonlinear oscillations in circuits and systems. IEEE Trans. Circuits Syst. 26, No.4, 235-254 (1979).

[9] Mees AI. Dynamics of feedback systems. Chichester, UK: John Wiley & Sons; 1981.

[10] Moiola JL, Chen G. Hopf bifurcation analysis - A frequency domain approach. Singapore: World Scientific Publishing Co.; 1996.

[11] Oppenheim AV, Schafer RW. Discrete-time signal processing. Englewood Cliffs: Prentice-Hall; 1989.

[12] Padín MS, Robbio FI, Moiola JL, Chen G. On limit cycle approximations in the van der Pol oscillator. Chaos Solitons Fractals 23, No.1, 207-220 (2005).

[13] Rand R, Armbruster D. Perturbations methods, bifurcation theory and computer algebra. New York: Springer-Verlag; 1987.

[14] Thompson JMT, Stewart HB. Nonlinear dynamics and chaos. Chichester. UK: John Wiley & Sons; 1986.

[15] Torrini G, Genesio R, Tesi A. On the computation of characteristic multipliers for predicting limit cycle bifurcations. Chaos Solitons Fractals 9, No.1-2, 121-133 (1998).

[16] Yu, P. Analysis on double Hopf bifurcation using computer algebra with the aid of multiple scales. Nonlinear Dyn. 27, No.2, 19-53 (2002).

Griselda R. Itovich
Departamento de Matemática, FAEA,
Universidad Nacional del Comahue,
Neuquén, Q8300BCX, Argentina.
gitovich@arnet.com.ar

Federico I. Robbio
Departamento de Ingeniería Eléctrica y de Computadoras
Universidad Nacional del Sur,
Bahía Blanca, B8000CPB, Argentina.
frobbio@uns.edu.ar

Jorge L. Moiola
Departamento de Ingeniería Eléctrica y de Computadoras
Universidad Nacional del Sur,
Bahía Blanca, B8000CPB, Argentina.
jmoiola@criba.edu.ar

Recibido: 1 de noviembre de 2005
Aceptado: 29 de agosto de 2006